arXiv:1601.04628v2 [cond-mat.mes-hall] 10 Sep 2016

A scheme to realize the quantum spin-valley Hall effect in monolayer graphene

SK Firoz Islam and Colin Benjamin*
National institute of Science education & Research, Bhubaneswar 751005, India

Quantum spin Hall effect was first predicted in graphene. However, the weak spin orbit interaction in graphene meant that the search for quantum spin Hall effect in graphene never fructified. In this work we show how to generate the quantum spin-valley Hall effect in graphene via quantum pumping by adiabatically modulating a magnetic impurity and an electrostatic potential in a monolayer of strained graphene. We see that not only exclusive spin polarized currents can be pumped in the two valleys in exactly opposite directions but one can have pure spin currents flowing in opposite directions in the two valleys, we call this novel phenomena the quantum spin-valley Hall effect. This means that the twin effects of quantum valley Hall and quantum spin Hall can both be probed simultaneously in the proposed device. This work will significantly advance the field of graphene spintronics, hitherto hobbled by the lack of spin-orbit interaction. We obviate the need for any spin orbit interaction and show how graphene can be manipulated to posses features exclusive to topological insulators.

I. INTRODUCTION

Graphene is the material of the 21st century, what Silicon was to the 80's and 90's. It continues to be the most exciting material in condensed matter today, although challenged by topological insulators, for it's ability to show some striking unusual phenomena and it's potential applications in nanoelectronics[1]. Several remarkable features of graphene, which are in complete contrast to semicon ductor heterostructures, are Klein tunneling[2] and room temperature quantum Hall effect[3]. It's electronic properties are governed by massless linear dispersion- Dirac behavior at low energy around two distinct valleys K and K' in it's Brillouin zone. These two valleys, connected by time reversal symmetry, can also act as an additional degree of freedom just like spin in spintronics[4]. Similar to spintronics, the valley degree of freedom can also be exploited as regards applications in quantum computation-referred as valleytronics[5–7]. In valleytronics proposals, via controlling the valley degree of freedom, valley based filter, valve and field effect transistor have been already reported[7–12]. There were also proposals of quantum spin valley Hall effect in multilayer graphene[13], spin-valley filter in graphene [14] and thermally driven spin and valley currents in Group-VI dichalcogenides[15].

An exciting aspect of graphene is that a mechanical strain provides an excellent way to control valley degree of freedom. Strain causes an opposite transverse velocity in the two valleys (K,K')[16, 17]. The separation in momentum space between two valleys, generated by the opposite velocity, causes the well known valley Hall effect[18, 19]. The various Hall effects possible in graphene are mentioned in the Box. Apart from strain, there are several other proposed schemes to produce valley polarization-like triangular wrapping effects[7], edge effects in graphene nanoribbons[20] and a valley dependent gap generated by substrate[21–23], etc. Strained graphene can also show some electro-optic properties like: total internal reflection, valley dependent Brewster angle and Goos Hanchen effects[24].

The possible Hall effects in monolayer graphene

Depending on the situation encountered one can have any or some of the following conditions satisfied in our proposed device:

Ia. $I_c^K = I_c^{K'} = 0$ ($I_\uparrow = -I_\downarrow$)- The condition of pure spin current generation in each valley regardless of the angle of incidence of electron. Here, $I_c^{K/K'} = I_{K/K'}^{\uparrow} + I_{K/K'}^{\downarrow}$, the total charge current in K/K' valley,

Ib. $I_c^K(\phi) = I_c^{K'}(\phi) = 0$- The condition of pure spin current generation in each valley at a particular angle of incidence ϕ.

II. $I_c^K(\phi) = -I_c^{K'}(\phi)$, charge currents are same and opposite in each valley for a particular angle of incidence-quantum valley Hall effect (QVH).

IIIa. $I_\uparrow^K(\phi) = -I_\downarrow^{K'}(\phi)$ with $I_\downarrow^K(\phi) = I_\uparrow^{K'}(\phi) = 0$ i.e; two valleys carrying opposite spin current with same magnitude but in opposite direction-quantum spin-valley Hall effect (QSVH) of 1st kind,

IIIb. $I_\downarrow^K(\phi) = -I_\uparrow^{K'}(\phi)$ with $I_\uparrow^K(\phi) = I_\downarrow^{K'}(\phi) = 0$-QSVH of 1st kind.

IV. $I_\uparrow^K(\phi) - I_\downarrow^K(\phi) = -[I_\uparrow^{K'}(\phi) - I_\downarrow^{K'}(\phi)]$, QVH with pure spin current in each valley. This can also be termed as QSVH of 2nd kind.

In the present work, we use the following symbols for different components of pumped currents: spin-up current: $I_\uparrow$, spin-down current: $I_\downarrow$, spin current: $I_s = I_\uparrow - I_\downarrow$ and charge current: $I_c = I_\uparrow + I_\downarrow$. Quantum spin-valley Hall effect (QSVH) is defined as one valley carries a current of only spin up (spin down) and the other valley carries a current of spin down (spin up) with same magnitude but in exactly opposite direction. A variant of this, i.e., two valleys carry pure spin currents in exactly opposite direction with same magnitude is termed as QSVH of 2nd kind, see Fig.1 for a pictorial on QVH and QSVH (first and second kinds). In this work, we aim to manipulate both degrees of freedom, i.e., spin and valley, for which we dope the graphene monolayer with a magnetic impurity and an electrostatic potential and also apply an in-plane strain to the graphene layer. We find that the condition (Ia) of pure spin current generation in each valley is satisfied in Fig. 7. The condition (Ib) of pure spin current generation at a particular angle of incidence and the QVH appear in Fig. 5(b) (upper panel). We get the condition (III) of QSVH of 1st kind in Fig. 4, while the condition (IV) of

* **Corresponding Author. Email: colin.nano@gmail.com**

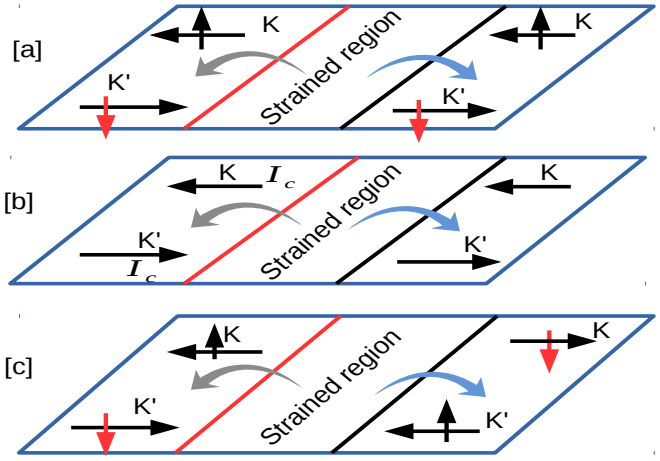

Figure 1. A pictorial representation of different possible charge/spin pumped currents in each valley. The red and black solid lines are two scatterers (magnetic impurity and delta potential). In Fig. 1(a), K and K' valley carry exclusively spin up and spin down currents in exactly opposite direction-quantum spin valley Hall effect (QSVH of 1st kind). Fig. (1b) shows charge currents in each valley are same in magnitude and opposite in direction-quantum valley Hall effect (QVH). Fig. (1c) shows pure spin currents in each valley are same and opposite in direction, we call it quantum valley Hall effect with pure spin current (QSVH of 2nd kind).

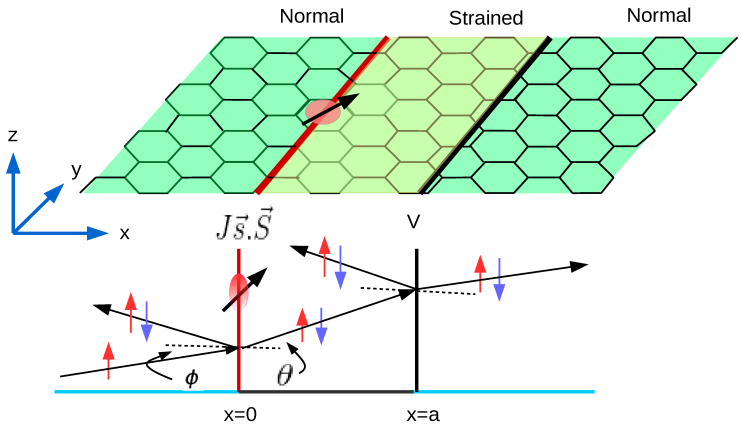

Figure 2. Top: The graphene layer with the red solid line representing the magnetic impurity at $x = 0$, while black line is for electrostatic delta potential at $x = a$. The interveneing portion is the strained region. Valley and spin dependent currents are pumped out of the strained region by modulating magnetic impurity and electrostatic potential. The lower picture shows incident up electron (for K-valley) is reflected/transmitted with or without spin flip by magnetic impurity. The angle of incidence is ϕ, while the angle of refraction into the strained region is θ for a particular valley. Similar phenomena occurs at the other interface with electrostatic delta potential without spin flip.

QSVH of 2nd kind is found in Fig. 5(b) (lower panel).

II. THEORY

Graphene is a two dimensional carbon allotrope with hexagonal lattice structure [1] that can be split into two triangular sublattices A and B. We consider a mechanical strain to be applied to the graphene sheet which is lying in the x-y plane[16, 17], in the region between magnetic impurity at $x = 0$ and electrostatic potential at $x = a$. The sketch of the considered system is shown in Fig. 2. Strain is included in the Dirac Hamiltonian as follows- In-plane mechanical strain affects the hopping amplitude between two nearest neighbors and can be described as a gauge vector which are opposite in two valleys. In the Landau gauge, the vector potential corresponding to the strain is $\mathbf{A} = (0, A_y)$. The system can be easily described by the Hamiltonian[24–26], as:

$$\mathcal{H}_{K/K'} = H_{K/K'} + J\mathbf{s}.\mathbf{S}\delta(x) + V\delta(x-a) \tag{1}$$

with $H_K = \hbar v_F \sigma.(\mathbf{k}-\mathbf{t})$ and $H_{K'} = \hbar v_F \sigma^*.(\mathbf{k}+\mathbf{t})$. Here, $t = \frac{A_y}{\hbar v_F}[\Theta(x) - \Theta(x-a)]$ is the strain with Θ being the step function, v_F is the Fermi velocity. The first term represents the kinetic energy for graphene with $\sigma = (\sigma_x, \sigma_y)$- the Pauli matrices that operate on the sublattices A or B and $\mathbf{k} = (k_x, k_y)$ the 2D wave vector. Second term is the exchange interaction between Dirac electron and magnetic impurity and final term is an electrostatic delta potential. In the second term J represents the strength of the exchange interaction which depends on the magnetization of the magnetic impurity and modulating it's magnetization one can effectively change J. The spin of Dirac electron is denoted by s, while S represents spin of the magnetic impurity. V is the strength of the potential, situated at $x = a$. Energy of the electron will be denoted by 'E'.

A short review of basic theory of quantum pumping and the method of solving the scattering problem for spin-up/down electron is given in the following sub-sections.

A. Quantum pumped currents

Adiabatic quantum pumping is a phenomena in which charge can be transported without any external bias. It requires cyclic variations of the scattering matrix, which could be realized by the periodic modulation of two independent system parameters of the device. The first experimental attempt at quantum pumping was done by M. Switkes in 1999[30], where the pumping signal was recorded in response to the cyclic deformation of the confining potential. Concurrently, P.W. Brouwer provided the theory of quantum pumping[31]. Pumping has also been used to generate spin dependent currents in theory[32] as well as experiments[33]. Recently, several theoretical works have been reported on quantum spin and valley current pumping in graphene based devices consisting of ferromagnet/valley dependent mass term and gate electrodes[34, 35]. To generate pure spin current, spin-up and spin-down currents have to be exactly same in magnitude and opposite in direction. Same goes for pure valley currents also. To calculate quantum pumped currents, we proceed as follows: The infinitesimal change of two system parameters, say ζ_i with $i = 1, 2$, causes an infinitesimal charge transport (dQ) through

the lead α(say)- in a particular valley(K) with spin (τ) is given by-

$$dQ_K^{\tau\alpha}(t) = e\sum_i \frac{dN_{\tau\alpha}}{d\zeta_i}\delta\zeta_i(t) \tag{2}$$

and the current transported in one period being-

$$I_k^{\tau\alpha} = \frac{ew}{2\pi}\int_0^{2\pi/w} dt \sum_i \frac{dN_{\tau\alpha}}{d\zeta_i}\frac{d\zeta_i}{dt}, \tag{3}$$

w being the frequency of applied modulation to parameters ζ_i. The quantity $dN_{\tau\alpha}/d\zeta_i$ is known as emissivity which can be obtained from the elements of the scattering matrix, in the zero temperature limit by-

$$\frac{dN_{\tau\alpha}}{d\zeta_i} = \frac{1}{2\pi}\sum_{\tau',\beta}\Im(\frac{\partial s_{\alpha\beta}^{\tau\tau'}}{\partial\zeta_i}s_{\alpha\beta}^{\tau\tau'*}). \tag{4}$$

Here $s_{\alpha\beta}^{\tau\tau'}$ represents the scattering matrix elements as denoted above, α and β take values 1 (for pumping to left of strained region) and 2 (for pumping to right of strained region), while τ,τ' are the spin indices, ↑ and ↓, depending on whether spin is up or down. The symbol "$\Im$" indicates the imaginary part of the complex quantity inside parenthesis. $s^{\tau\tau'}$ indicates scattering amplitudes when incident electron with spin index τ' is scattered (reflected or transmitted) to the state in spin index τ. The individual spin pumped currents are generated by adiabatically modulating the magnetization of impurity 'J' and the strength of the electrostatic "delta" potential V, herein $\zeta_1 = J = J_0 + J_p\sin(wt)$ and $\zeta_2 = V = V_0 + V_p\sin(wt+\Omega)$. w as before is the frequency of modulation and Ω is the phase difference between the two modulated parameters. A section on the feasibility of experimental realization of the proposed device is given in the conclusion.

The line integral of Eq. (3) can be converted into an surface integral by using Stokes theorem on two dimensional plane. Then after some straight forward manipulation, for sufficiently weak pumping ($\delta\zeta_i \ll \zeta_i$), we have (see for details [32]),

$$I_K^{\tau\alpha}(\phi) = \frac{ew\delta\zeta_1\delta\zeta_2\sin(\Omega)}{2\pi}\sum_{\beta=1,2}\Im(\frac{\partial s_{\alpha\beta}^{\tau\tau'*}}{\partial\zeta_1}\frac{\partial s_{\alpha\beta}^{\tau\tau'}}{\partial\zeta_2}). \tag{5}$$

Weak pumping is defined by: $J_p \ll J_0, V_p \ll V_0$, and Eq. 5 reduces to-

$$I_K^{\tau\alpha}(\phi) = I_0\sum_{\tau'=\uparrow,\downarrow,\beta=1,2}\Im(\frac{\partial s_{\alpha\beta}^{\tau\tau'*}}{\partial J}\frac{\partial s_{\alpha\beta}^{\tau\tau'}}{\partial V}), \text{wherein } I_0 = \frac{ewJ_pV_p\sin(\Omega)}{2\pi} \tag{6}$$

For parameter values $e = 1.6X10^{-19}$ Coulombs, $w = 10^8$ Hertz from Ref.[30], I_0 is of the order of $J_pV_p10^{-11}$ Amperes, with J_p and V_p again defined as above but in their dimensionless form. Since we are in the weak pumping regime we can consider J_p and V_p to be each around 0.1 as in Figs. 5-9 we have taken $J = 2V = 2eV - nm$, this makes $I_0 = 10^{-13}$ Amperes. We are considering pumped spin currents into lead 1 (left of strained region), therefore $\alpha = 1$ throughout this paper. In the above equation, if we consider pumped currents in K valley to left of strained region then $alpha = 1$ with spin $\tau = \uparrow$ then different scattering amplitudes are denoted by-

$s_{11}^{\uparrow\uparrow} \equiv r_{\uparrow\uparrow}$, $s_{11}^{\uparrow\downarrow} \equiv r_{\uparrow\downarrow}$, $s_{12}^{\uparrow\uparrow} \equiv t'_{\uparrow\uparrow}$, and $s_{12}^{\uparrow\downarrow} \equiv t'_{\uparrow\downarrow}$, where

$r_{\uparrow\uparrow}$: reflection amplitude for spin-up electron reflected to the spin-up state,

$r_{\uparrow\downarrow}$: reflection amplitude for spin-down electron reflected to the spin-up state,

$t'_{\uparrow\uparrow}$: transmission amplitude for spin-up electron transmitted to the spin-up state, and

$t'_{\uparrow\downarrow}$: transmission amplitude for spin-down electron transmitted to the spin-up state.

Similarly, we can calculate the spin down current by replacing $\uparrow\rightarrow\downarrow$ and vice-versa.

Here, $s_{\alpha\beta}^{\tau\tau'*}$ is complex conjugate of $s_{\alpha\beta}^{\tau\tau'}$. After taking integration over ϕ, the total spin-up/down pumped current in a K-valley becomes:

$$I_K^{\tau} = \int_{-\pi/2}^{\pi/2} I_K^{\tau}(\phi)\cos(\phi)d\phi. \tag{7}$$

Similarly, For K' valley we get pumped current by replacing $t \rightarrow (-t)$ and $k_y \rightarrow (-k_y)$ in the Hamiltonian, Eq. (1) and wavevectors Eqs. (9,10) below. The pumped currents in each valley of course depend on the incident angle as well as energy of the electron.

Effect of finite temperature:

So far we confined our discussion at zero temperature. The effects of any non-zero temperature could be easily absorbed by multiplying a factor $[-df(E)/dE]$ with $I_K^{\tau}(\phi)$ and integrating over electron energy[36] as-

$$I_K^{\tau}(\phi) = \int_0^{\infty}\big[-\frac{df(E)}{dE}\big]I_K^{\tau}(\phi)dE, \tag{8}$$

where $\tau = \uparrow,\downarrow$, and $f(E)$ is the Fermi-Dirac distribution function.

B. The scattering problem: Wave functions and boundary conditions

Let us consider the case of a spin-up electron with energy E, scattered from magnetic impurity at an incidence angle of ϕ. The electron can be reflected or transmitted to spin-up/down electron. We shall start with the inclusion of disorder in the system. We have modeled the system in such way that the two independent system parameters (magnetic impurity and electrostatic delta potential) are at the two ends of the system, where disorder is randomly distributed in the strained region. We also assume that randomly distributed potentials are loclaized in $x-$direction but extended along $y-$direction, i.e., superlattice type potential.

The strength of random potentials are taken in the range of $100-150$ meV-nm. To obtain the scattering amplitudes, we

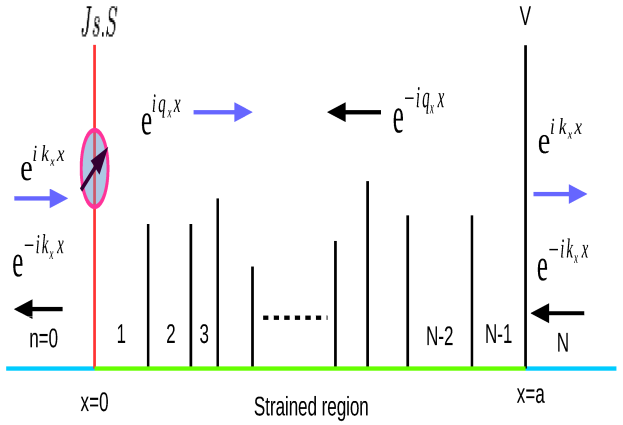

Figure 3. Randomly distributed disorder potentials with random strength are confined between two system parameters i.e J and V which are adiabatically modulated.

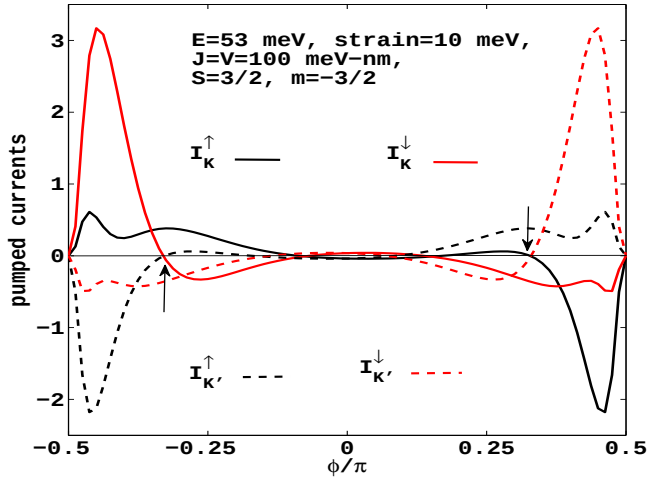

Figure 4. Quantum pumped spin up/down currents vs angle of incidence in each valley. Black arrow signs are used to indicate the quantum spin-valley Hall effect, i.e; $I_K^{\downarrow} = -I_{K'}^{\uparrow}$ while $I_K^{\uparrow} = I_{K'}^{\downarrow} = 0$ at a particular angle of incidence, QSVH of first kind.

shall adopt the transfer matrix approach. Transfer matrix connects the wave function amplitudes between left and right of the scatterer. The wave function for A-sublattice in each strained region for K-valley can be written as:

$$\psi_n^A(x) = (A_n^{\uparrow}e^{iq_x x} + B_n^{\uparrow}e^{-iq_x x})\chi_{\frac{1}{2}}\xi_m + (A_n^{\downarrow}e^{iq_x x} + B_n^{\downarrow}e^{-iq_x x})\chi_{-\frac{1}{2}}\xi_{m+1}. \quad (9)$$

and for B-sublattice

$$\psi_n^B(x) = (A_n^{\uparrow}e^{iq_x x+i\theta} - B_n^{\uparrow}e^{-iq_x x-i\theta})\chi_{\frac{1}{2}}\xi_m + (A_n^{\downarrow}e^{iq_x x+i\theta} - B_n^{\downarrow}e^{-iq_x x-i\theta})\chi_{-\frac{1}{2}}\xi_{m+1}. \quad (10)$$

Here $n = 1, 2, 3...(N-1)$ corresponding to different regions bounded by the delta potentials, as shown in Fig. 3. The x-component of the momentum vector inside the strained region: $q_x = \sqrt{(E/\hbar v_F)^2 - (k_y - t)^2}$. For the unstrained region i.e; "$n = 0$" and "$n = N$", q_x has to be replaced by k_x, where $k_x = E\cos\phi/(\hbar v_F)$. The phase factor inside the strained region is defined by $\tan\theta = (k_y - t)/q_x$. ξ_m is the eigen state of z-component of spin operator of magnetic impurity S_z, $S_z\xi_m = m\xi_m$ with m being the corresponding eigen value. The scattering mechanism is considered as elastic and the z-component of the total spin remains conserved. Following the Refs.[37–39], we obtain the boundary conditions at the location of two independent time dependent system parameters J and V as:
at $x = 0$:

$$-i\hbar v_F[\psi_1^B(x=0) - \psi_0^B(x=0)] = \frac{J}{2}\mathbf{s}.\mathbf{S}[\psi_1^A(x=0) + \psi_0^A(x=0)] \quad (11)$$

and

$$-i\hbar v_F[\psi_1^A(x=0) - \psi_0^A(x=0)] = \frac{J}{2}\mathbf{s}.\mathbf{S}[\psi_1^B(x=0) + \psi_0^B(x=0)] \quad (12)$$

.

at $x = a$:

$$-i\hbar v_F[\psi_N^B(x=a) - \psi_{N-1}^B(x=a)] = \frac{V}{2}[\psi_N^A(x=a) + \psi_{N-1}^A(x=a)] \quad (13)$$

and

$$-i\hbar v_F[\psi_N^A(x=a) - \psi_{N-1}^A(x=a)] = \frac{V}{2}[\psi_N^B(x=a) + \psi_{N-1}^B(x=a)] \quad (14)$$

.

Before proceeding further, we shall mention that spin flipping process is attributed to the interaction term between the spin of electron (s) and the spin of magnetic impurity (S), $\mathbf{s}.\mathbf{S} = s_z S_z + (1/2)(s^-S^+ + s^+S^-)$as: $s^-S^+\begin{bmatrix}1\\0\end{bmatrix}\xi_m = F\begin{bmatrix}0\\1\end{bmatrix}\xi_{m+1}$ and $s^+S^-\begin{bmatrix}0\\1\end{bmatrix}\xi_m = F'\begin{bmatrix}1\\0\end{bmatrix}\xi_{m-1}$ with $F = \sqrt{(S-m)(S+m+1)}$ and $F' = \sqrt{(S+m)(S-m+1)}$. Here, s_z and S_z are the z-components of the spin operator of electron and magnetic impurity, respectively. $S^{\pm} = S_x \pm iS_y$ are the raising and lowering operators for magnetic impurity, and $s^{\pm} = s_x \pm is_y$ are the same for conduction electron.

Following the boundary condition prescribed in Eqs.(11)-(14), the transfer matrix across the magnetic impurity (at $x = 0$) i.e., between region "$n = 0$" and "$n = 1$" as in Fig. 3 is given as-

$$\begin{bmatrix}A_1^{\uparrow}\\A_1^{\downarrow}\\B_1^{\uparrow}\\B_1^{\downarrow}\end{bmatrix} = \mathcal{M}^{[1,0]}\begin{bmatrix}A_0^{\uparrow}\\A_0^{\downarrow}\\B_0^{\uparrow}\\B_0^{\downarrow}\end{bmatrix}, \quad (15)$$

where $\mathcal{M}^{[1,0]}$, transfer matrix across magnetic impurity, given

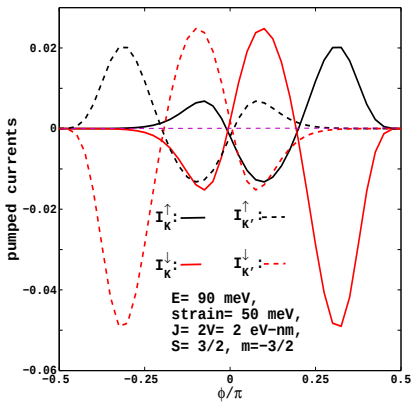

(a) Quantum pumped spin up/down currents in each valley Vs. angle of incidence of electron. Spin up current ($I_\uparrow$) or spin down current $I_\downarrow$) in either valley is flowing in opposite direction for a wide range of ϕ.

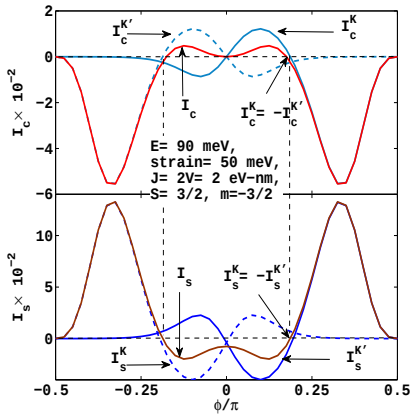

(b) Quantum pumped charge (upper panel) and spin (lower panel) currents in each valley Vs. angle of incidence. Here, $I_{c/s} = I^K_{c/s} + I^{K'}_{c/s}$. The upper panel shows that charge currents in both valleys are same in magnitude and flow in exactly opposite direction-QVH, while the lower panel shows the same for spin currents-QSVH of 2nd kind.

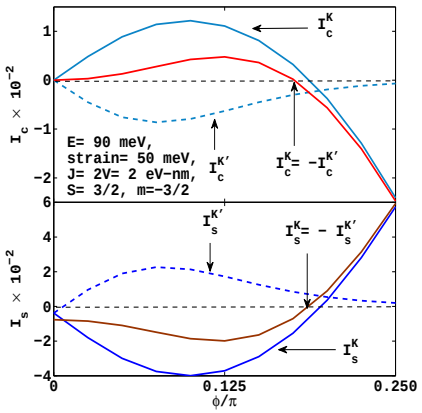

(c) Zoomed portion of (0-$\pi/4$) of Fig. (4b) is shown here. The upper panel shows the QVH while lower panel shows the QSVH of 2nd kind.

Figure 5. Pumped spin-valley currents

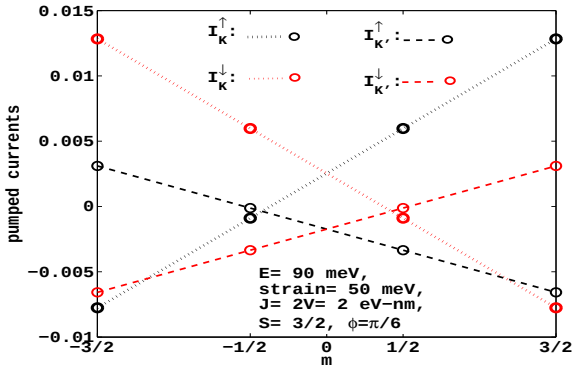

(a) Quantum pumped spin up/down currents in each valley Vs. m for $S = 3/2$. Parameters are taken as in Fig.5 at an angle of incidence $\phi = \pi/6$ around which QVH (condition II) and QSVH(2nd kind) (condition IV) are met when $m = -3/2$.

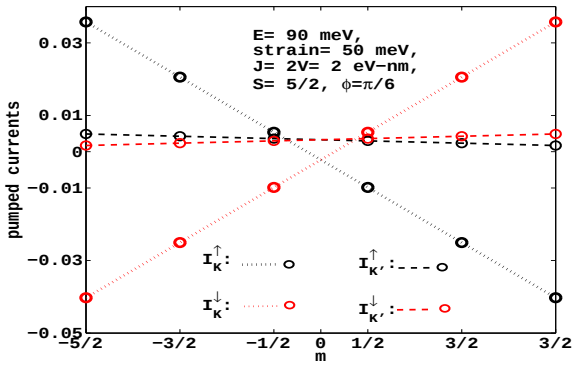

(b) Quantum pumped spin up/down currents Vs m for $S = 5/2$. Though same parameters are used as in Fig.5 except $S = 5/2$, but $I^\uparrow_K$ ($I^\downarrow_K$) and $I^\uparrow_{K'}$($I^\downarrow_{K'}$) flow in the same direction.

Figure 6. Quantum pumped spin up/down currents in each valley Vs. magnetic quantum number (m). with different S for a particular angle of ϕ.

by $\mathcal{M}^{[1,0]} = \mathcal{M}_0^{-1}\mathcal{M}_1$ with

$$\mathcal{M}_0 = \begin{bmatrix} \bar{\xi} - iJ'm & -iJ'F & iJ'm - \bar{\xi}_c & -iJ'F \\ -iJ'F & \bar{\xi} + iJ'(m+1) & -iJ'F & -iJ'(m+1) - \bar{\xi}_c \\ 1 - iJ'm\bar{\xi} & -iJ'F\bar{\xi} & 1 + iJ'm\bar{\xi}_c & iJ'F\bar{\xi}_c \\ -iJ'F\bar{\xi} & 1 + iJ'(m+1)\bar{\xi} & iJ'F\bar{\xi}_c & 1 - iJ'(m+1)\bar{\xi}_c \end{bmatrix} \tag{16}$$

and

$$\mathcal{M}_1 = \begin{bmatrix} \xi + iJ'm & iJ'F & iJ'm - \xi_c & iJ'F \\ iJ'F & \xi - iJ'(m+1) & iJ'F & -iJ'(m+1) - \xi_c \\ 1 + iJ'm\xi & iJ'F\xi & 1 - iJ'm\xi_c & -iJ'F\xi_c \\ iJ'F\xi & 1 - iJ'(m+1)\xi & -iJ'F\xi_c & 1 + iJ'(m+1)\xi_c \end{bmatrix} \tag{17}$$

with $\bar{\xi} = \exp(i\theta)$ and $\bar{\xi}_c = \exp(-i\theta)$, $\xi = \exp(i\phi)$ and $\xi_c = \exp(-i\phi)$. Also, $J' = J/(2\hbar v_F)$. Similarly, the transfer-matrix between "$n = N$" and "$n = N-1$" at $x = a$, is

$$\begin{bmatrix} A^\uparrow_N \\ A^\downarrow_N \\ B^\uparrow_N \\ B^\downarrow_N \end{bmatrix} = \mathcal{M}^{[N,N-1]} \begin{bmatrix} A^\uparrow_{N-1} \\ A^\downarrow_{N-1} \\ B^\uparrow_{N-1} \\ B^\downarrow_{N-1} \end{bmatrix}, \tag{18}$$

where $\mathcal{M}^{[N,N-1]}$ is the transfer matrix across any disorder po-

tential, expressed as $\mathcal{M}^{[N,N-1]} = \mathcal{M}_{N-1}^{-1}\mathcal{M}_N$ with

$$\mathcal{M}_{N-1} = \begin{bmatrix} \xi - iV' & 0 & iV' - \xi_c & 0 \\ 0 & \xi - iV' & 0 & iV' - \xi_c \\ 1 - iV'\xi & 0 & 1 + iV'\xi_c & 0 \\ 0 & 1 - iV'\xi & 0 & 1 + iV'\xi_c \end{bmatrix}, \quad (19)$$

and

$$\mathcal{M}_N = \begin{bmatrix} \bar{\xi} + iV' & 0 & iV' - \bar{\xi}_c & 0 \\ 0 & \bar{\xi} + iV' & 0 & iV' - \bar{\xi}_c \\ 1 + iV'\bar{\xi} & 0 & 1 - iV'\bar{\xi}_c & 0 \\ 0 & 1 + iV'\bar{\xi} & 0 & 1 - iV'\bar{\xi}_c \end{bmatrix}. \quad (20)$$

Here, $V' = V/(2\hbar v_F)$. Since electrostatic potential at x=a (acting as a system parameter) and disorder potential are both modeled as delta function potential, the transfer- matrix for any arbitrary interface between $x = 0$ and $x = a$ has also the same matrix elements as $\mathcal{M}^{[N,N-1]}$. After some straight forward algebraic manipulation, we construct the total transfer-matrix which connect s the wave function amplitudes of extreme left and right as[38]

$$\begin{bmatrix} A_N^{\uparrow} \\ A_N^{\downarrow} \\ B_N^{\uparrow} \\ B_N^{\downarrow} \end{bmatrix} = \mathcal{M} \begin{bmatrix} A_0^{\uparrow} \\ A_0^{\downarrow} \\ B_0^{\uparrow} \\ B_0^{\downarrow} \end{bmatrix}, \quad (21)$$

where

$$\mathcal{M} = \mathcal{M}^{[N,N-1]}\mathcal{M}_{free}^{[N-1]}\mathcal{M}^{[N-1,N-2]}\mathcal{M}_{free}^{[N-2]}.....\mathcal{M}_{free}^{[1]}\mathcal{M}^{[1,0]} \quad (22)$$

with $\mathcal{M}_{free}^{n}$ being the propagation matrix between any two successive disorder potential, which is given by

$$\mathcal{M}_{free}^{n} = \begin{bmatrix} e^{iq_x d_n} & 0 & 0 & 0 \\ 0 & e^{iq_x d_n} & 0 & 0 \\ 0 & 0 & e^{-iq_x d_n} & 0 \\ 0 & 0 & 0 & e^{-iq_x d_n} \end{bmatrix} \quad (23)$$

with d_n is the spatial gap between two successive disorder potentials. Also, $\mathcal{M}^{[N,N-1]}$ is the transfer-matrix which connect the wave function amplitudes between the regions “N-1" and “N". To calculate the reflection and transmission amplitudes, we shall use the relation between scattering matrix and transfer-matrix as [38]

$$S = \frac{1}{\mathcal{M}_{22}} \begin{bmatrix} \mathcal{M}_{21} & I \\ I \det \mathcal{M} & \mathcal{M}_{12} \end{bmatrix}, \quad (24)$$

with

$$\mathcal{M} = \begin{bmatrix} \mathcal{M}_{11} & \mathcal{M}_{12} \\ \mathcal{M}_{21} & \mathcal{M}_{22} \end{bmatrix} = \begin{bmatrix} m_{11} & m_{12} & m_{13} & m_{14} \\ m_{21} & m_{22} & m_{23} & m_{24} \\ m_{31} & m_{32} & m_{33} & m_{34} \\ m_{41} & m_{42} & m_{43} & m_{44} \end{bmatrix}, \quad (25)$$

as is obvious from Eq. (25), $I, \mathcal{M}_{11}, \mathcal{M}_{12}, \mathcal{M}_{21}, \mathcal{M}_{22}$ are all 2×2 matrices. The reflection amplitude (to the left, as we are calculating pumping current in the left lead)

$$r = -\frac{\mathcal{M}_{21}}{\mathcal{M}_{22}} = \begin{bmatrix} r_{\uparrow\uparrow} & r_{\uparrow\downarrow} \\ r_{\downarrow\uparrow} & r_{\downarrow\downarrow} \end{bmatrix} \quad (26)$$

and transmission amplitude from right to left is

$$t = \frac{1}{\mathcal{M}_{22}} = \begin{bmatrix} t_{\uparrow\uparrow} & t_{\uparrow\downarrow} \\ t_{\downarrow\uparrow} & t_{\downarrow\downarrow} \end{bmatrix}. \quad (27)$$

The scattering amplitudes obtained by the above method can be directly used in Eq. (6) to obtain the quantum pumping current. Now we can recover the situation of disorder free pumped current by using transfer matrix as $\mathcal{M} = \mathcal{M}^{[2,1]}\mathcal{M}_{free}^{1}\mathcal{M}^{[1,0]}$, where $\mathcal{M}^{[2,1]}$ and $\mathcal{M}^{[1,0]}$ would become the transfer-matrix across the electrostatic potential and magnetic impurity, respectively. And, d_1 would become a in Eq. (23). By solving this scattering problem numerically, we obtain different scattering amplitudes which obey probability conservation $\mid t_{\uparrow\uparrow} \mid^2 + \mid r_{\uparrow\uparrow} \mid^2 + \mid t_{\downarrow\uparrow} \mid^2 + \mid r_{\downarrow\uparrow} \mid^2 = 1$ for a particular angle of incidence ϕ and for particular spin (here, $\uparrow$) incident. In experiment, graphene electrons can be incident at a particular angle by means of beam collimation techniques (discussed in conclusion also). To focus graphene electron at particular angle without any spatial spreading, periodic potential can be used suitably as proposed by Park, et. al., in Ref.[29].

Similarly for the case of spin-down incident electron from the left side, we can get scattering amplitudes. This procedure can be repeated appropriately for spin-up/down electron coming from right side. We repeat this for for K'-valley by chosing $t \to (-t)$ and $k_y \to (-k_y)$ in the Hamiltonian and corresponding wavefunctions.

III. RESULTS AND DISCUSSION

To calculate pumped current for different spin components, we use the formula- Eq. (6) of Theory section. First, we have plotted different components of spin pumped currents (in units of I_0) i.e; spin-up ($I_\uparrow$), spin-down ($I_\downarrow$), spin current ($I_s = I_\uparrow - I_\downarrow$) and charge current ($I_c = I_\uparrow + I_\downarrow$), in K and K' valley, shown in Fig. 4.

We have chosen parameters: the spatial separation between the magnetic impurity and the electrostatic delta potential $a =$ 40 nm, spin of the molecular magnet $S = 3/2$, and $m = -3/2$ in all figures 4-9. Here, m is the eigen value of S_z, the z-component of the spin operator of magnetic impurity. Other parameters are mentioned in the figures.

In Fig. 4, we see that at a particular angle of incidence, one valley carries spin up current while other valley carries spin down current with same magnitude but in opposite direction. We notice that around $\phi = \pi/3$, $I_{K'}^{\downarrow} = I_K^{\uparrow} = 0$ but $I_{K'}^{\uparrow} = -I_K^{\downarrow}$, satisfying condition (IIIa)-QSVH of 1st kind. Similarly around $\phi = -\pi/3$, we see $I_{K'}^{\uparrow} = I_K^{\downarrow} = 0$ but $I_K^{\uparrow} = -I_{K'}^{\downarrow}$, satisfying the condition (IIIb)-QSVH of 1st kind.

The spin current I_s and charge current I_c corresponding to Fig. 5(a) are shown in Fig. 5(b). In the upper panel of Fig. 5(b), we find that charge current in K and K'-valley are same in magnitude but opposite in direction, satisfying the condition (II) i.e; quantum valley Hall effect (QVH). The lower panel of Fig. 5(b) shows that spin current in K and K'-valley are same but opposite in direction, satisfying the condition (IV) i.e; quantum spin-valley Hall effect (QSVH) of 2nd kind. A zoomed portion

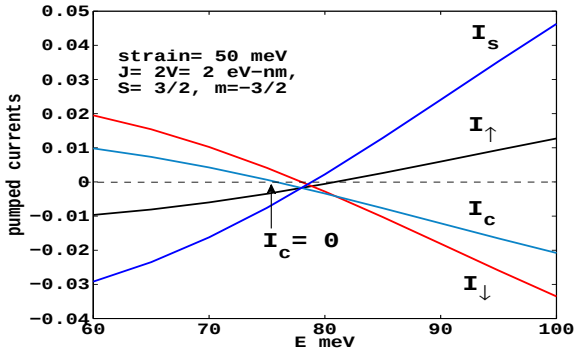

(a) Pumped currents in each valley after integration over angle from $-\pi/2$ to $\pi/2$ (here, $I_K = I_{K'}$ because of the time reversal symmetry). There is pure spin current, satisfying the condition (Ia).

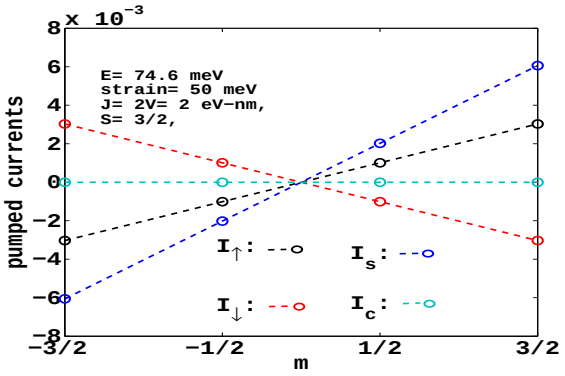

(b) Pumped currents Vs m for $S = 3/2$ after integrating over angle of incidence. We use parameters as in Fig(7a) at $E = 74.6$ meV where Condition (Ia) is satisfied.

Figure 7. Quantum pumped currents in each valley Vs. magnetic quantum number (m).

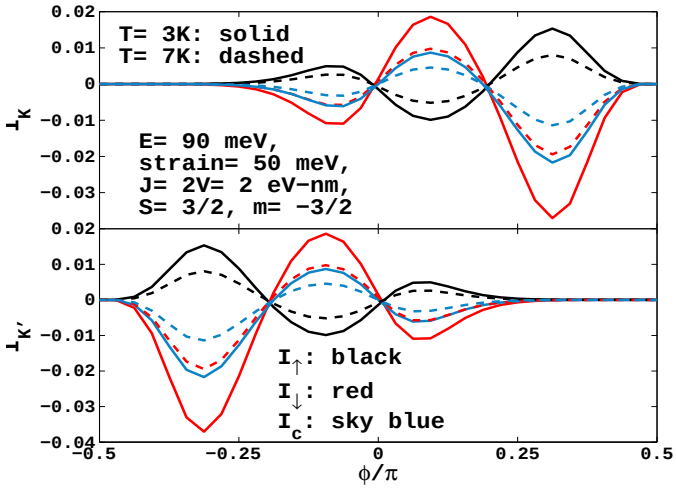

Figure 8. Effect of temperature on pumped current in each valley Vs angle of incidence.

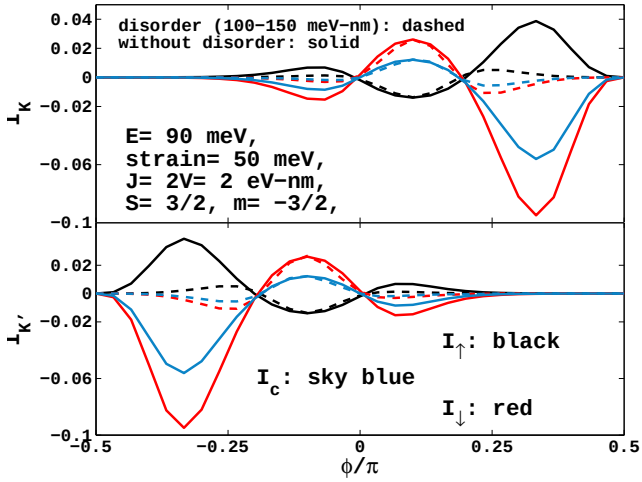

Figure 9. Effect of disorder on pumped currents Vs angle of incidence.

(0-$\pi/4$) of Fig. 5(b) is given in Fig. 5(c). For $S = 3/2$, there are four possible values of m $(-3/2, -1/2, 1/2, 3/2)$. In Fig.6(a), we show how different components of quantum pumped current varies with m for a particular angle $\phi = \pi/6$. Similar plot is also given for $S = 5/2$ in Fig. 6(b), which indicates that pumped currents are very sensitive to m.

We also consider the case of all angle incidence, i.e., we integrate over the angle of incidence ϕ in Eq.(7), we plot pumped currents versus energy in Fig. 7(a). Because of the time reversal symmetry, pumped currents in both valleys would be identical. Here, we see that pure spin current appears at a certain energy satisfying the condition (Ia). In the Fig. 7(b), it is shown that we get a pure spin current regardless of the m value, satisying condition 1a of box.

Effect of temperature and disorder on QSVH:

Temperature has a very significant influence on transport properties, especially on the magnitude of transport coefficients. Here, we look at how temperature can affect the pumped spin valley currents. We plot pumped currents versus the angle of incidence for two different non-zero temperatures in Fig. 8, for which we used Eq. (8). It is found that pumped currents are damped with increase in temperature, however the location of QVH or QSVH remains intact, temperature cannot shift the incidence angle ehere QVH or QSVH occur.

The study of disorder effects on transport properties has been always important, as disorder is always present in the electronic system. Here, we intend to examine how pumped currents get affected by random potential. For this, we treat the random potentials as delta like potential and solved the scattering problem by transfer matrix approach and then use Eq. (6) to calculate the pumped currents. The presence of randomly distributed impurities/adatoms/vacancies modeled by the delta potentials in the system can suppress the pumped currents which is shown in Fig. 9. We find that magnitude of pumped

currents are damped due to the presence of randomness, but again no change in the location where QSVH appears. However, very strong disorder may lead to the non-trivial changes. A tabular representation of our findings is given below:

Figure(↓) (Condition→)	QVH (II)	pure spin current in each valley (Ib/Ia)	QSVH of 1st kind (IIIa/IIIb)	QSVH of 2nd kind (IV)
4	——	——-	present	——
5b	present	present (Ib)	absent	present
7	——	present (Ia)	——	——
8 and 9	same as 5b but damped	same as 5b but damped	same as 5b but damped	same as 5b but damped

Table I. Summary of the results

IV. EXPERIMENTAL REALIZATION AND CONCLUSIONS

The 1D electrostatic delta potential can be realized by placing a series of several adatoms which can be adiabatically modulated by a gate voltage. This potential is acting as a system parameter only, it has nothing to do with spin/valley degree of freedom, so one can also use a thin rectangular potential barrier instead of delta potential. The 1D chain of magnetic impurity with $S = 3/2$ can be used as the other system parameter, experimental feasibility of these kind of wires is already established[27, 28]. The strength of exchange interaction can be varied by tuning the magnetic field of a ferromagnet placed on top of the magnetic chain. As we have shown that QSVH or QVH is observable at a particular angle of electron incidence, focusing of electron at particular angle is very important which can be realized by means of beam collimation[29]. The propagation of graphene electron beam without any spatial spreading or diffraction can be experimentally realized by applying 1D spatial periodic potential, here no external magnetic or electric field is required. This is called super beam collimator[29]. The phenomena of super beam collimation is described as follows- Under the influence of 1D periodic potential, group velocity of low energy graphene carriers becomes anisotropic. By suitably controlling the 1D potential, the extreme anisotropy in velocity can be realized giving us electrons on demand at a particular angle of incidence.

In conclusion, we have proposed a graphene based device to observe quantum spin valley Hall effect by adiabatically modulating a magnetic impurity and an electrostatic potential embedded in a monolayer of strained graphene. In the same device, we have also shown the appearance of quantum valley Hall effect, pure spin current generation in each valley and quantum valley Hall effect with pure spin current (QSVH of 2nd kind). We also examined the effects of temperature and disorder on pumped currents. In future, this work will be extended further to study the spin-valley dependent electro-optic like phenomena in strained graphene.

[1] Neto A. H. C., Guinea F., Peres N. M. R, Novoselov K. S., & Geim A. K., The electronic properties og graphene, Rev. Mod. Phys. 81, 109 (2009) and the references therein.

[2] Katsnelson M. I., Novoselov K. S., & Geim A. K., Chiral tunneling and the Klein paradox in graphene, Nature Physics 2, 620 - 625 (2006).

[3] Novoselov k. s., Jiang Z., Zhang Y., Morozov S.V., Stormer H.L, Zeitler U., Maan J.C., Boebinger G. S., Kim P., & Geim A. K., Room-Temperature Quantum Hall Effect in Graphene Science, 315, 1379 (2007); Zhang Y., Tan Y., Stormer H. L.,& Kim P., Experimental observation of the quantum Hall effect and Berry's phase in graphene, Nature 438, 201 (2005).

[4] Zutic I., Fabian J., & Sarma S. D., Spintronics: Fundamentals and applications, Rev. Mod. Phys. 76, 323(2004).

[5] Xiao D., Yao W., & Niu Q., Valley-Contrasting Physics in Graphene: Magnetic Moment and Topological Transport, Phys. Rev. Lett. 99, 236809 (2007).

[6] Pereira V. M., & Neto A. H. C., Strain Engineering of Graphene's Electronic Structure, Phys. Rev. Lett. 103, 046801 (2009).

[7] Rycerz A., Tworzyd J.,& Beenakker C. W. J., Valley filter and valley valve in graphene, Nature Phys. 3, 172 (2007).

[8] Lee M. K. , Lue N. Y., Chen Y. C. , Wen C. K.,& Wu G. Y., Valley-based FETs in graphene, arxiv 1208.0064

[9] Mak K. F., McGill K. L., Park J., & McEuen P. L., The valley Hall effect in MoS2 transistors, Science, 344, 1489 (2014).

[10] Xu X., Yao W.„ Xiao D.,& Heinz T. F., Spin and pseudospins in layered transition metal dichalcogenides, Nat. Phys. 10, 343 (2014).

[11] Isberg J., Gabrysch M., Hammersberg J., S. Majdi S., Kovi K.,& Twitchen D. J., , Generation, transport and detection of valley-polarized electrons in diamond, Nat. Mat. 12, 760 (2013).

[12] Zhai F. and Yang L., Strain-tunable spin transport in ferromagnetic graphene junctions, Appl. Phys. Lett. 98, 062101 (2011).

[13] Zhang F., Jung J., Fiete G. A., Niu Q., & MacDonald A. H., Spontaneous Quantum Hall States in Chirally Stacked Few-Layer Graphene Systems, Phys. Rev. Lett. 106, 156801 (2011).

[14] Marko M. G., Tadic M. Z., & Peeters F. M., Spin-Valley Filtering in Strained Graphene Structures with Artificially Induced Carrier Mass and Spin-Orbit Coupling, Phys. Rev. Lett. 113, 046601 (2014).

[15] Yu X. Q., Zhu Z., Gang S., & Jauho A. P., Thermally Driven Pure Spin and Valley Currents via the Anomalous Nernst Effect in Monolayer Group-VI Dichalcogenides, Phys. Rev. Lett. 115, 246601 (2015).

[16] Bao W. Z., Miao F., Chen Z.„ Zhang H.„ Jang W.„ C. Dames C.,& Lau C. N., Controlled ripple texturing of suspended graphene and ultrathin graphite membranes, Nat. Nanotech. 4, 562 (2009).

[17] Guinea F.„ Katsnelson M. I., & Geim A. K., Energy gaps and a zero-field quantum Hall effect in graphene by strain engineering, Nature Phys. 6, 30 (2009).

[18] Jiang Y., Low T., Chang K, Katsnelson M. I., & F. Guinea F., Generation of Pure Bulk Valley Current in Graphene, Phys. Rev.

Lett. 110, 046601 (2013).
[19] Low T., Jiang Y., Katsnelson M. I., & Guinea F., Electron Pumping in Graphene Mechanical Resonators, Nano Lett. 12, 850 (2012).
[20] Zhang Z. Z., Chang K.& Chan K. S., Resonant tunneling through double-bended graphene nanoribbons, Appl. Phys. Lett. 93, 062106 (2008).
[21] Peters E. C., Giesbers A. J. M., Zeitler U., Burghard M., & Kern K., Valley-polarized massive charge carriers in gapped graphene, Phys. Rev. B 87, 201403 (2013).
[22] Zhai F. and Chang K., Valley filtering in graphene with a Dirac gap, Phys. Rev. B 85, 155415 (2012).
[23] Moldovan D., Masir M. R., Covaci L., & Peeters F. M., Resonant valley filtering of massive Dirac electrons, Phys. Rev. B 86, 115431 (2012).
[24] Wu Z., Zhai F., Peeters F. M., Xu H. Q., & Chang K., Valley-Dependent Brewster Angles and Goos-Hanchen Effect in Strained Graphene, Phys. Rev. Lett. 106, 176802 (20011).
[25] Pereira V. and Neto A. H. C, Strain Engineering of Graphene's Electronic Structure, Phys. Rev. Lett. 103, 046801 (2009).
[26] Yang M. and Wang J., Fabry-Perot states mediated quantum valley-Hall conductance in a strained graphene system, New J. Phys. 16, 113060 (2015).
[27] Jaroszynski J., et. al. ,Influence of s-d Exchange Interaction on Universal Conductance Fluctuations in Cd_{1-x}Mn_xTe:In, Phys. Rev. Lett. 75, 3170 (1995).
[28] Ray O., Sirenko A. A., Berry J J., Samarth N., Gupta J. A, Malajovich I. & Awschalom D. D., Exciton spin polarization in magnetic semiconductor quantum wires, Appl. Phys. Lett. 76, 1167 (2000); H. Ikada, et al.,Photonics Spectra 10, 373 (2001).
[29] Park C. H., Son Y., Yang L., Cohen M. L, Louie S. G., Electron Beam Supercollimation in Graphene Superlattices, Nano Lett.,8, 2920 (2008).
[30] Switkes M., Marcus C. M., Campman K., & Gossard A. C., An Adiabatic Quantum Electron Pump, Science 283, 1905 (1999).
[31] Brouwer P. W., Scattering approach to parametric pumping, Phys. Rev. B 58, R10135 (1998).
[32] Benjamin R. and Benjamin C., Quantum spin pumping with adiabatically modulated magnetic barriers, Phys. Rev. B 69, 085318 (2004).
[33] Watson S. K., Potok R. M., Marcus C. M. & Umansky V., Experimental Realization of a Quantum Spin Pump, Phys. Rev. Lett. 91, 258301 (2003).
[34] Zhang Q., Chang K. S. & Lin Z. , Spin current generation by adiabatic pumping in monolayer graphene, Appl. Phys. Lett. 98, 032106 (2011); Zhang Q., Chang K.S., & Lin Z. , Pure spin current generation in monolayer graphene by quantum pumping, J. Phys.: Condens. Matter 24, 075302 (2012);
[35] Wang J., Chan K.& Lin Z., Quantum pumping of valley current in strain engineered graphene, Appl. Phys. Lett. 104, 013105 (2014); Wang J., Lin Z.& Chan K., Pure valley current generation in graphene with a Dirac gap by quantum pumping, Appl. Phys. Exp. 7, 125102 (2014).
[36] Moskalets M. and Buttiker M., Floquet scattering theory of quantum pumps, Phy. Rev. B 66, 205320 (2002).
[37] Menezes O. L. T. and Helman J. S., Spin flip enhancement at resonant transmission, Am. J. Phys. 53, 1100 (1985).
[38] Griffths D. J. and Steinke C. A., Waves in locally periodic media, Am. J. Phys. 69, 137 (2001).
[39] Maruri G. C, Omar Y., de Coss R. & Bose S., Graphene-enabled low-control quantum gates between static and mobile spins, Phys. Rev. B 89, 075426 (2014).

ACKNOWLEDGEMENTS

This work was supported by funds from Dept. of Science and Technology (Nanomission), Govt. of India, Grant No. SR/NM/NS- 1101/2011. Authors thank Arjun Mani, School of Physical Sciences, NISER, Bhubaneswar for useful discussions.

V. COMPETING FINANCIAL INTERESTS STATEMENT

Authors have no competing financial interests to disclose.